Binding of Volatile Anesthetics to Serum Albumin: Measurements of Enthalpy and Solvent Contributions

Abdul H. Sawas,[‡,§] Srinivas N. Pentyala,[*,‡,||] and Mario J. Rebecchi[*,‡,||]

Departments of Anesthesiology, Pharmacology, and Physiology and Biophysics, School of Medicine, State University of New York, Stony Brook, New York 11794

Received October 30, 2003; Revised Manuscript Received July 20, 2004

ABSTRACT: This study directly examines the enthalpic contributions to binding in aqueous solution of closely related anesthetic haloethers (desflurane, isoflurane, enflurane, and sevoflurane), a haloalkane (halothane), and an intravenous anesthetic (propofol) to bovine and human serum albumin (BSA and HSA) using isothermal titration calorimetry. Binding to serum albumin is exothermic, yielding enthalpies (ΔH_{obs}) of −3 to −6 kcal/mol for BSA with a rank order of apparent equilibrium association constants (K_a values): desflurane > isoflurane ∼ enflurane > halothane ≥ sevoflurane, with the differences being largely ascribed to entropic contributions. Competition experiments indicate that volatile anesthetics, at low concentrations, share the same sites in albumin previously identified in crystallographic and photo-cross-linking studies. The magnitude of the observed ΔH increased linearly with increased reaction temperature, reflecting negative changes in heat capacities (ΔC_p). These $-\Delta C_p$ values significantly exceed those calculated for burial of each anesthetic in a hydrophobic pocket. The enhanced stabilities of the albumin/anesthetic complexes and $-\Delta C_p$ are consistent with favorable solvent rearrangements that promote binding. This idea is supported by substitution of D_2O for H_2O that significantly reduces the favorable binding enthalpy observed for desflurane and isoflurane, with an opposing increase of ΔS_{obs}. From these results, we infer that solvent restructuring, resulting from release of water weakly bound to anesthetic and anesthetic-binding sites, is a dominant and favorable contributor to the enthalpy and entropy of binding to proteins.

The molecular basis of general anesthesia is one of the long-standing puzzles of medical science. General anesthetic agents include compounds as varied as the noble gases, alkanes, alcohols, and ethers (*1*−*3*). Although varied in structure, all volatile anesthetics are moderately hydrophobic, have a small dipole moment, and fit the positive Meyer−Overton correlation between anesthetic potency and oil or lipid-phase solubility, with few exceptions. This suggests that most of the functional target sites within the central nervous system are "oily" in nature. Because of their high solubility in lipid, these compounds can reach concentrations on the order of 50−100 mM in biological membranes, where, because of their amphipathic nature, they tend to localize at the interface between the polar headgroup region and the hydrophobic core of phospholipid bilayers (*4*). These characteristics have led previous investigators to infer that volatile anesthetics alter the physical properties of the membrane and thereby perturb its excitability, a hypothesis that still has its proponents (*5*, *6*).

More recently, the emphasis has shifted from theories of lipid perturbation to the idea that general anesthetics bind directly to specific proteins (*3*, *7*−*10*). The physiologic targets of volatile agents remain controversial, but enough evidence has accumulated to suggest that ligand-gated ion channels, such as the γ-aminobutyric acid $(GABA)_A$ and glycine receptors (*8*), and a few soluble proteins, such as PKC (*11*), are candidates.

Specific mutations in the $GABA_A$ and glycine receptors (*8*) provide support for the concept that anesthetics occupy pre-existing cavities formed between the transmembrane helices of these allosteric proteins (*9*, *10*). These small voids are thought to accommodate the conformational changes associated with ligand gating. Filling these cavities with volatile or gaseous anesthetics may prevent or alter these processes by repopulating existing conformers. Studying the direct interactions of volatile anesthetics with ion channels, however, has been exceptionally difficult because of their low affinity and the inability to obtain the most relevant protein targets in sufficient quantities; therefore, most previous studies have involved indirect measurements, typically a perturbation of ion-channel activity.

To understand the physicochemical basis for anesthetic protein interactions, more abundant soluble proteins have served as models (*3*, *9*). Of these, serum albumin contains a number of cavities that bind a wide array of amphipathic hormones, metabolites, and pharmaceuticals. Because of its properties and abundance, serum albumin has become the best-studied model of general anesthetic binding. Direct binding measurements have involved photoaffinity affinity

* To whom correspondence should be addressed. E-mail: mrebecchi@notes.cc.sunysb.edu. Telephone: (631) 444-8178. Fax: (631) 444-2907 (M.J.R.). E-mail: srinivas.pentyala@stonybrook.edu. Telephone: (631) 444-2974. Fax: (631) 444-2907 (S.N.P.).

‡ Department of Anesthesiology.

§ Department of Pharmacology.

|| Department of Physiology and Biophysics.

10.1021/bi035941d CCC: $27.50
Published on Web 09/08/2004

labeling (*12*−*14*), intrinsic fluorescence (*15*, *16*), nuclear magnetic resonance (NMR) (*17*, *18*), and zonal elution chromatography (*16*, *19*). These studies demonstrate that halothane, isoflurane, and other volatile anesthetics bind to several "high" and multiple low-affinity sites and are consistent with recent crystallographic structures that show halothane binding to three such "high" affinity sites, one of which is shared by the intravenous anesthetic, propofol (*20*). These sites resemble the putative cavities identified in $GABA_A$ and glycine receptors. Further supporting this idea, soluble helical bundles, resembling the transmembrane helices, can be artificially engineered to create comparable hydrophobic pockets that bind halothane with affinities spanning the clinical concentration range (*21*).

The predominantly oily nature of the hydrophobic cavities in serum albumin (*20*) suggest that anesthetic binding from aqueous solution is driven by short-range electrostatic (van der Waals) interactions and by increased solvent disorder. Indeed, the anesthetic, chloroform, binds to bovine serum albumin (BSA) with the release of heat, consistent with an important enthalpic contribution arising from van der Waals attraction (*22*). The present study examines the enthalpy and entropy of binding of closely related haloethers (desflurane, isoflurane, enflurane, and sevoflurane), a haloalkane (halothane), and an intravenous anesthetic (propofol) binding to BSA and human serum albumin (HSA), using isothermal titration calorimetry (ITC). The effects of temperature on binding, which yields the change in heat capacity (ΔC_p) and isotopic solvent substitution are used to address the role of the solvent. When these data are coupled with structural information, they provide new insights into the nature of anesthetic-binding free energies.

MATERIALS AND METHODS

Materials. Anesthetics used in these experiments were halothane, 2-bromo-2-chloro-1,1,1-trifluoroethane (Halocarbon Laboratories); sevoflurane, fluoromethyl-2,2,2-trifluoro-1-(trifluoromethyl)ethyl ether (Abbot Laboratories); isoflurane, 1-chloro-2,2,2-trifluoroethyl difluoromethyl ether (Ohmeda PPD Inc.); enflurane, 2-chloro-1,1,2-trifluoroethyl difluoromethyl ether (Ohmeda PPD Inc.); desflurane, 2-difluoromethyl-1,2,2,2-tetrafluoroethyl ether (Baxter); and pure propofol, 2,6-bis(1-methylethyl)phenol (Astra Zeneca). D_2O (99.9%) was from Cambridge Isotope Laboratories, Inc., MA. BSA and HSA (fatty acid free), guanidine hydrochloride, and all other reagents were from Sigma Chemical Co.

Measurement of Anesthetic and Protein Concentrations. The aqueous concentrations of each drug (C_{aq}) were determined by sampling the gaseous headspace and calculated using the Ostwald water/gas partition coefficients (λ) appropriate to each temperature and drug, as described earlier (*23*). The concentrations of propofol in the aqueous solution are calculated by measuring the absorbance at 270 nm, using $\epsilon = 1584\ M^{-1}\ cm^{-1}$. Protein concentrations were determined by absorbance at 280 nm using the molar extinction coefficient of 40 000 $M^{-1}\ cm^{-1}$.

ITC Measurements. BSA or HSA was dissolved in buffer (150 mM NaCl and 10 mM HEPES at pH 7.2), to a protein concentration of 0.15 mM. To ascertain the contributions of buffer ionization enthalpy, parallel measurements were obtained by substituting phosphate buffer (NaH_2PO_4 at pH 7.2), for HEPES. Pure liquid volatile anesthetics were mixed with degassed buffer and were allowed to equilibrate with the aqueous phase in Teflon-sealed glass vials by gentle mixing overnight. Concentrations of the drugs in the saturated buffer solutions were determined by gas chromatography as described earlier (*23*). Working solutions of propofol were prepared by mixing the pure drug with buffer in a glass tube that was then centrifuged at 1000*g* for 5 min at room temperature. The aqueous layer was separated and used for the study. Calorimetric measurements were carried out at 10−35 °C in an isothermal titration calorimeter (VPITC, MicroCal, MA). The anesthetic agents, protein sample, and buffers, with the exception of solutions containing volatile agents, were extensively degassed before each titration. The drug solution (titrant) was loaded into the syringe, and the BSA or HSA solution was introduced into the cell (1.43 cm^3). Binding was measured by titrating the anesthetic into the continuously stirred protein solution (reversing this order gave similar results). The instrument was programmed to introduce a set volume of drug (typically 10 μL) into the cell to a total of 300 μL with a time interval of 2−3 min between each injection to allow for equilibration. Isolation of the cell from the atmosphere by a narrow column of unstirred fluid (6 cm in height) helped preserve the level of injected volatile anesthetic and allowed the recovery of >90% of the volatile agents tested after 2 h of titration at atmospheric pressure.

The heat released or absorbed (Q) upon each injection was measured, and the values obtained from a parallel titration of anesthetic into buffer without protein provided a baseline to subtract the heat of dilution for each titration step. The data were plotted as integrated quantities ΔQ_i, the change in heat content of the solution following ith injections, and analyzed with a single class, noninteractive binding site model using the Origin software supplied by MicroCal. For a single class of site, the following relationship was fit to the data:

$$Q_i = n\theta M_t \Delta H V_0 \tag{1}$$

where Q_i is the total heat content of the solution following the ith injection (from the integrated heat pulses), n is the number of ligands bound to the single class of sites, θ is the fractional ligand occupancy, which is related to K, the apparent association constant, in units of M^{-1}, M_t is the total concentration of protein, ΔH is the enthalpy of binding per mole of ligand, and V_0 is the initial working volume of the calorimeter cell.

Q_i is related to ΔQ_i, the integrated heat pulses by

$$\Delta Q_i = Q_i + \mathrm{d}\, V/V_0[Q_i + Q_{i-1}/2] - Q_{i-1} \tag{2}$$

$$Q_i = nM_t\Delta HV_0/2[1 + L/nM_t + 1/nKM_t - ((1 + L/nM_t + 1/nKM_t)^2 - 4L/nM_t)^{1/2}] \tag{3}$$

where Q_{i-1} is the total heat content prior to the ith injection and L_i is the total concentration of the ligand after the ith injection. The standard state was taken as an aqueous solution of free ligand at 1 M concentration.

Desflurane binding data were also analyzed using two classes of independent binding sites: a high affinity class of stoichiometry, $n = 1$, and a low affinity class, $n = 2$.

This model defines the equilibrium association constants as

$$K_1 = \theta_1/(1 - \theta_1)L \quad (4)$$

$$K_2 = \theta_2/(1 - \theta_2)L \quad (5)$$

$$L_t = L + M_t(n_1\theta_1 + n_2\theta_2) \quad (6)$$

where L_t = the total ligand concentration and

$$L_t = L + n_1M_tLK_1/1 + LM_t + n_2M_tLK_2/1 + LK_2 \quad (7)$$

Numerical solutions for L are obtained using Newton's Method by assigning values for n_1, n_2, K_1, and K_2. θ_1 and θ_2 are then solved in eqs 4 and 5. The heat content Q after any injection i is then expressed as

$$Q_i = M_tV_0(n_1\theta_1\Delta H_1 + n_2\theta_2\Delta H_2) \quad (8)$$

ΔQ_i is then calculated after the correction for displaced volume (eq 2).

Binding models were fit to the data by a nonlinear least-squares Marquardt algorithm until constant χ^2 values were achieved. ΔS was deduced from K and ΔH using the definition of the Gibbs free-energy difference (ΔG) and its relationship to K. The significance of differences of the thermodynamic parameters between anesthetics was assessed by one-way ANOVA analysis and Newman−Keuls multiple comparisons test.

Changes in heat capacities (ΔC_p) were estimated from the linear least-squares slopes of the ΔH values, determined at temperatures ranges between 10 and 35 °C measured in 5 °C increments, and plotted as a function of temperature. Data from multiple determinations were used, and linear least-squares analysis was performed that included a test for the departure from linearity.

Isotopic Solvent Substitution and ITC Measurements. Fatty acid free BSA from the same batch was weighed and dissolved in carefully matched D_2O or H_2O buffer (150 mM NaCl and 10 mM HEPES at pD or pH 7.2), to a final protein concentration of 0.15 mM, which was checked by absorbance at 280 nm. The difference in pH electrode response was compensated as described previously (*24*), and the pD and pH of the two solutions were adjusted to equivalence. Volatile anesthetics were mixed with D_2O or H_2O buffer and allowed to equilibrate in Teflon sealed glass vials by gentle mixing overnight. Concentrations of the drugs in saturated buffer solution were determined by gas chromatography. These calorimetric measurements were carried out at 20 °C.

Calculations of ΔC_p and Lipole Moments. Predicted values of ΔC_p were estimated for each compound using the molecular modeling program, VEGA (*25*), the minimum free-energy structures for each anesthetic, and its empirical relation to hydrophobic surface area as previously described (*26*, *27*). Lipole moments, analogous to dipolar momentum and comparable to hydrophobic moment (*28*, *29*) were determined using this same molecular modeling program, the minimum free-energy structures for each anesthetic, and the relation

$$\text{(lipole moment) } L = \sum_i r_i\, l_i \quad (9)$$

where r_i is the distance between atom i and the specified origin of the molecule and l_i is the lipophilicity of atom i.

Fluorescence Measurements of Protein Stability. Fluorescence measurements were performed with a spectrofluorometer (model: I.S.S. K2, ISI, Champaign, IL). The protein solutions (with or without drugs) were transferred into quartz cuvettes with Teflon stoppers that permitted filling with little headspace volume. The fluorescence spectra were measured with a 1-cm path-length continuously stirred cell at 20 °C. Excitation and emission bandwidths were set at 4 nm. Intrinsic fluorescence was measured by exciting the stirred protein solution at 290 nm (to favor tryptophan excitation), and emission spectra were recorded in the wavelength range of 305−380 nm.

Stock solutions of protein and the denaturant, guanidinium hydrochloride (GdmHCl), were prepared in 150 mM NaCl and 10 mM HEPES at pH 7.2. For denaturation experiments, different volumes of 6 M GdmHCl were mixed with a protein solution to obtain a final concentration of 0.1 μM protein, 2.5 mM drug, and the desired concentration of GdmHCl (0.25−3 M) in a final volume of 4.2 mL in the quartz cuvette. Incubation for at least 1 min was allowed to equilibrate the drug with the protein. The intensity values did not change significantly with time indicating that the system was at equilibrium. The intensity data were normalized to fluorescence intensity obtained in the absence of the denaturant (F_{max}), whereas the minimal intensity was defined in the presence of a [GdmHCl] that completely denatured the protein (F_{min}). Because the changes in fluorescence intensity failed to conform to a simple two-state model of native and denatured protein, a sigmodial dose response relation with variable slope was fit to the data and used to estimate the midpoints of the titration curves. Significant differences between the transition midpoints from at least three independent titrations were determined by Student t test with Bonferroni corrections for multiple comparisons.

RESULTS

The energetics of anesthetic binding to serum albumin were assessed using an isothermal titration calorimeter (VPITC, MicroCal), which measures the heat produced or absorbed during the binding reaction. We examined several closely related volatile haloethers, isoflurane, enflurane, desflurane, and sevoflurane, to defatted BSA and HSA. Isoflurane differs from desflurane only by the substitution of chlorine for fluorine at a single position; and enflurane is a chemical isomer of isoflurane; and the most distinctive feature of sevoflurane is its branched chain trifluoromethyl group. Also tested were the haloalkane, halothane, and the intravenous anesthetic, propofol, two drugs for which direct molecular information was available (*20*).

Injection of aqueous drug solutions into a range of serum albumin concentrations (0.01−0.67 mM) produced raw heat pulse data (D_p in μcal/s) with downward (negative) deflections, which indicated that the anesthetic binding to either BSA or HSA is exothermic. Binding was reversible, because the curves could be reproduced following degassing to remove volatile agents from the recovered protein (not shown). Examples of BSA (0.15 mM) titrated with enflurane (top) and desflurane (bottom) are presented in Figure 1 and insets. As the concentrations of drugs were increased, the associated

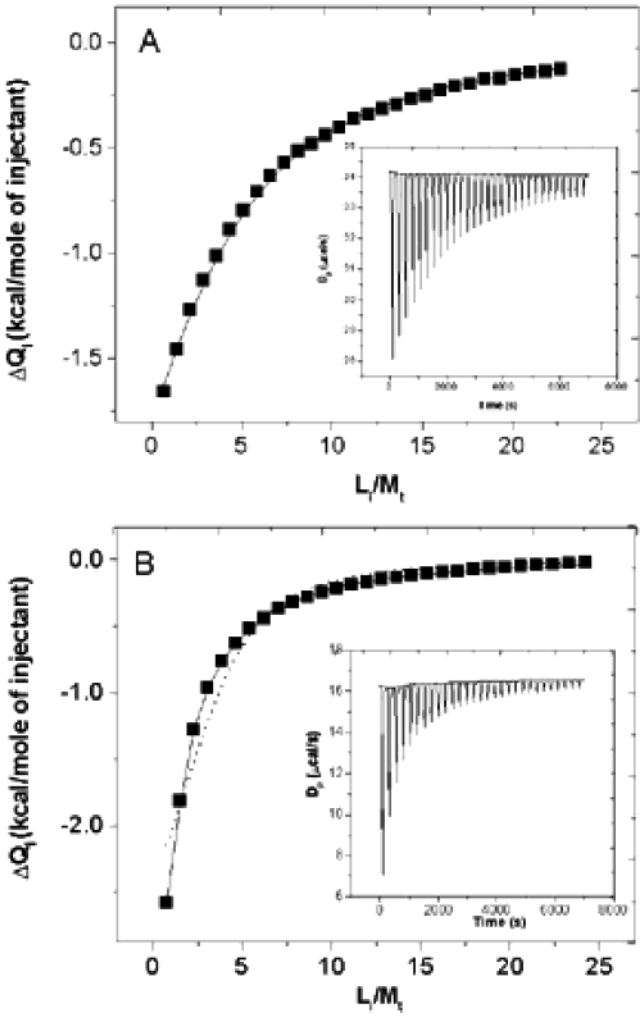

FIGURE 1: Binding of enflurane and desflurane to defatted BSA as measured by ITC. (Inserts) Raw heat pulse data (μcal/s) generated on injections of 10 μL of a 16 mM solution of desflurane (A) or 15 mM enflurane (B) into 1.437 mL of 0.15 mM BSA, 2 min apart, at 20 °C (inset traces and calculated baselines). (Main illustration) Heat pulses of the inset were baseline-subtracted and integrated, and the heat of dilution of the drug into buffer was subtracted. The corrected ΔQ_i values (■) were plotted as a function the mole ratio of enflurane (A) or desflurane (B) to BSA. In A, the solid curve represents the best fit to eq 1, a single class of noninteracting binding sites ($n = 3$). In B, the solid curve represents the best nonlinear least-squares fit to a two classes of site model, eq 8 ($n_1 = 1$ and $n_2 = 2$), whereas the dotted curve is the best fit to eq 1 ($n = 3$).

heat pulses (insets) closely approached the corresponding signals obtained from diluting the individual volatile anesthetics into buffer lacking protein (with the exception of sevoflurane). The integrated heat pulse data (parts A and B of Figure 1) are expressed as kcal/mol of titrant (ΔQ_i) and plotted as a function of the mole ratio of drug/protein (L_i/M_t). A standard nonlinear least-squares regression model of binding, involving a single class of noninteracting sites (eq 1), is fit to the data (solid curve in A and dotted curve in B). The nonsaturable low-affinity sites were not included in the analysis (<2.5% of the initial power signals obtained titrating desflurane, isoflurane, or enflurane). Parallel titrations of anesthetic diluted into buffer lacking protein were used to determine the corresponding ΔQ_i contributed by the heat of dilution of the anesthetics. These values (<0.03 kcal/mol) were subtracted from serum albumin titration curves.

While binding stoichiometry was >1:1, small differences in affinities among multiple sites reduced the sigmoidal character of the integrated heat pulse data, greatly increasing the confidence intervals (CIs) for estimation of n and therefore the other parameters. Moreover, to accurately determine the inflection point (n), the concentrations of enflurane, halothane, and sevoflurane, as well as the protein required would have exceeded their solubility. In the case of desflurane and isoflurane, however, accurate midpoint determinations were obtained at high serum albumin (0.67 mM) concentrations (Table 1).

Binding to defatted serum albumin has been measured previously by a variety of independent methods. Estimates of the number of "high-affinity" halothane-binding sites were obtained by chromatography ($n \sim 2$ mol of anesthetic/mol of albumin) (*19*), photo-cross-linking ($n \geq 2$) (*13*), and X-ray crystallography ($n = 3$) (*20*). ^{19}F NMR measurements of high-affinity isoflurane binding yielded $n \sim 4$ (*17*). Our estimates of desflurane and isoflurane binding agree well with these results (Table 1). It was recently reported that BSA binds approximately 7.6 mol of halothane per mol of HSA (*62*). However, the reported n value has an error of determination of ±5.7. Thus, $n = 3$ mol of volatile anesthetic/mol of serum albumin appears the most consistent approximation for saturable binding at the drug concentrations examined here.

Binding to enflurane (Figure 1A), was fit well to a simple single class of noninteracting sites $n = 3$ (eq 1). Increasing n to 4 or decreasing it to 2 did not significantly improve the fits of the binding model. To facilitate comparisons among the drugs, other titration data were also analyzed using this model (summarized in Table 1). Desflurane, however, was better fit with two classes of noninteracting sites, a single high-affinity ($n_1 = 1$) and two low-affinity sites ($n_2 = 2$) (solid curve in Figure 1B compared to the dotted curve, $n = 3$), summarized in Table 2.

Fits to the single class, noninteracting site model yielded the single apparent equilibrium association constants (K values) and the binding enthalpies and entropies (Table 1). Results are pooled from similar values obtained at 15 and 150 μM serum albumin. For binding to BSA, the rank order of K is desflurane > isoflurane ~ enflurane > halothane ≥ sevoflurane at 20 °C, corresponding to apparent equilibrium dissociation constants of 0.340−3.40 mM. Binding to HSA is comparable with some differences, with the most notable being the higher affinity of isoflurane and enflurane ($K \sim$ 1.5−1.7-fold higher). Binding of sevoflurane is of the lowest affinity; its binding constant was not well-determined. The apparent binding enthalpies of ΔH_{obs} to BSA ranged from −3046 to −6238 cal/mol, with the rank order being halothane ~ enflurane > sevoflurane > isoflurane ~ desflurane. While the $-T\Delta S$ values contributed favorably to binding of desflurane and isoflurane, the entropic contributions were unfavorable for enflurane and halothane. Similar results were obtained for HSA. Titration of propofol, in the range accessible in aqueous solutions (up to ~0.8 mM), yielded an n of 1.2−1.4.[1] In all cases, binding is driven primarily by the favorable enthalpic changes, although the increments in K and the corresponding increments in ΔG are best explained by the positive correlation with $-T\Delta S$ (Figure 2).

Table 1: Thermodynamic Parameters of Anesthetic Binding to BSA and HSA[a]

	BSA					
	desflurane	isoflurane	enflurane	halothane	sevoflurane	propofol
n (mol/mol)	2.6 (2.2−2.9)	3.2 (2.1−4.3)	3	3	3	1.4 ± 0.005
K (M^{-1})	2935 ± 953	1339 ± 123	877 ± 135	398 ± 53	268 ± 37	6959 ± 728
ΔH (cal/mol)	−3046 ± 545	−3954 ± 388	−5981 ± 249	−6238 ± 401	−4303 ± 2244	−5663 ± 315
$T\Delta S$ (cal/mol)	1576 ± 371	238 ± 439	−2012 ± 290	−2752 ± 468	−1049 ± 2322	−4416 ± 1107
ΔG (cal/mol)	−4622	−4192	−3969	−3486	−3254	−5052
ΔC_p measured	−78 ± 2	−103 ± 4	−191 ± 24	−193 ± 5	−904 ± 354	
95% CI ΔC_p	−104 to −52	−115 to −92	−288 to −94	−269 to −119	−3129 to +1321	
ΔC_p predicted	34	7	−5	−27	30	
	HSA					
	desflurane	isoflurane	enflurane	halothane	sevoflurane	propofol
n (mol/mol)	3.5 (3.4−3.7)	3	3	3	3	1.2 ± 0.09
K (M^{-1})	3707 ± 297	2019 ± 168	1498 ± 110	444 ± 20	549 ± 372	2680 ± 691
ΔH (cal/mol)	−3684 ± 554	−3737 ± 70	−5267 ± 80	−4864 ± 99	−1699 ± 675	−15420 ± 6194
$T\Delta S$ (cal/mol)	1102 ± 589	696 ± 118	−1005 ± 122	−1311 ± 19	1899 ± 1104	−15654 ± 4349
ΔG (cal/mol)	−4786	−4433	−4262	−3553	−3598	−4466

[a] Apparent association constants K and the binding enthalpies ΔH were determined at 20 °C from fits to the data of a single class, noninteracting binding sites model (eq 1). The results are presented as the mean ± SD of multiple titrations. Binding stoichiometry n (95% CI) was determined from the desflurane and isoflurane titration midpoints of one class of sites model as described (see the Materials and Methods). For the other volatile anesthetics, $n = 3$ was held constant. ΔC_p (cal mol^{-1} K^{-1}) are obtained from linear regression slopes of the ΔH plotted as a function of temperature in the range of 10−35 °C (± standard errors of determination). CI ΔC_p are CIs for the slopes of the least-squares linear regressions. ΔC_p predicted are estimated using the empirical relation to the buried hydrophobic and polar surface areas (see the Materials and Methods).

Table 2: Binding of Desflurane to BSA Modeled as High- and Low-Affinity Class Sites

affinity (class)	n	K (M^{-1})	ΔH (cal/mol)	$T\Delta S$ (cal/mol)	ΔG (cal/mol)	ΔC_p (cal mol^{-1} K^{-1})
high	1	28 700 ± 1330	−3285 ± 715	2655 ± 920	−5940	−132 ± 49
low	2	1474 ± 205	−3560 ± 430	702 ± 448	−4262	−63 ± 2

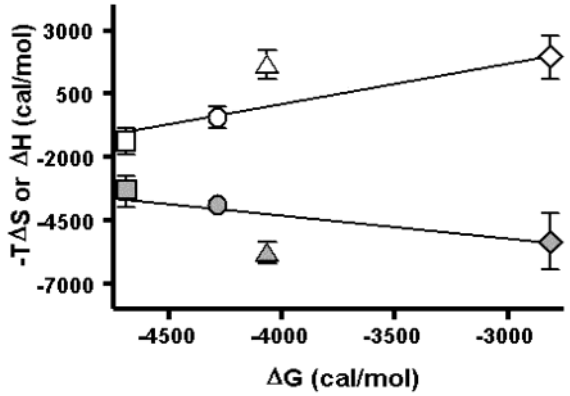

FIGURE 2: Relation of the thermodynamic parameters ΔH and $-T\Delta S$ to ΔG of binding. Thermodynamic parameters ± standard deviation (SD) were determined from multiple titrations of BSA and HSA with desflurane (□ and ■), isoflurane (○ and ●), enflurane (△ and ▲), and halothane (◇ and ◆). $-T\Delta S$ values are represented by open symbols, and ΔH values are represented by filled symbols. The calculated linear regression slopes are -0.91 ± 0.23 ($r^2 = 0.34$) and 1.63 ± 0.24 ($r^2 = 0.63$) for ΔH and $-T\Delta S$, respectively. Slopes are significantly different from 0 with $p < 0.001$.

Although these anesthetics have no formal charges and are not ionized under our conditions, it was possible that protein conformational changes induced by the drugs may lead to changes of the protein ionization state through the release or absorption of protons. Such a change should be reflected in the ionization state of the buffer. To address this issue, we compared the ΔH values obtained in HEPES to those measured in phosphate, two buffers with quite different enthalpies of ionization (~7 and 0.7 kcal/mol). We found the ratios of ΔH observed in HEPES and phosphate buffers to be 0.94, 1.04, and 0.96 for desflurane, isoflurane, and enflurane, respectively. Therefore, changes in the ionization state of the albumin with a subsequent change in the buffer ionization are not detected upon binding of these anesthetics.

To test whether these agents bind overlapping sites, we performed competition experiments in which the protein is titrated with one drug to near saturation, followed by titration with another. Previous results using ^{19}F NMR of isoflurane (*17*) or photo-cross-linking of radio-labeled halothane (*14*) had shown that isoflurane, halothane, and enflurane bind to the same sites. Our data are consistent with this conclusion. In the presence of 2.5 mM halothane, binding of isoflurane, enflurane (Figure 3A), and sevoflurane (not shown) are nearly abolished, demonstrating that mutual binding is not possible. (Figure 3B).

Because propofol overlaps only one of the sites for halothane in HSA (*20*), this intravenous drug should only partly inhibit the binding of halothane and desflurane. Our results are consistent with this prediction (Figure 4A). The heat pulses, measured in the low concentration ranges of the two volatile agents (<1 mM), are partly suppressed at 0.16 mM propofol. On the other hand, because propofol binds to only one site under these conditions, high concentrations of halothane or desflurane should completely inhibit the binding of propofol, which they do (Figure 4B). Similar results were obtained with isoflurane, enflurane, and sevoflurane (not shown). At saturating aqueous propofol concentrations (0.82 mM), we found that exothermic heat pulses, caused by the binding of desflurane to BSA, were greatly reduced (Figure 5). This reduction corresponded mainly to the high-affinity

[1] While this manuscript was under review, Liu et al. reported that binding of propofol to HSA is exothermic and primarily enthalpy driven (*62*). They find a higher stoichiometry for binding of propofol ($n = 1.7$). They also report a higher K for binding of propofol to HSA. The reason for this discrepancy is unclear.

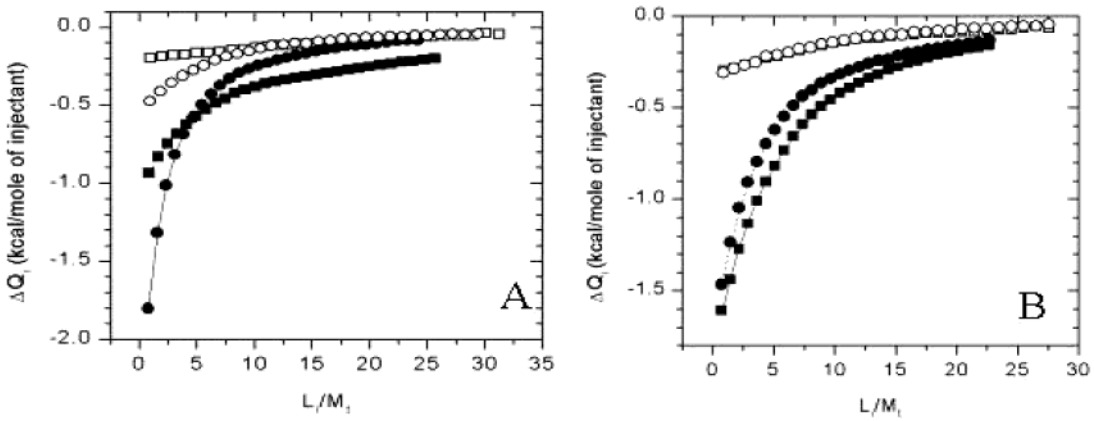

FIGURE 3: Binding of volatile anesthetics and their mutual inhibition. (A) ΔQ_i values of binding of halothane (■) and desflurane (●) are plotted as functions of the mole ratio of drug/BSA. After the complete titration of either halothane or desflurane to 2.9 and 2.7 mM, respectively, a second syringe filled with an aqueous solution of the competing drug halothane (□) or desflurane (○) was then used to titrate the BSA. (B) Similar experiments were performed with isoflurane, enflurane, and halothane. Isoflurane (○ and ●) or enflurane (□ and ■) was titrated before (filled symbols) or after (open symbols) the addition of 2.9 mM halothane.

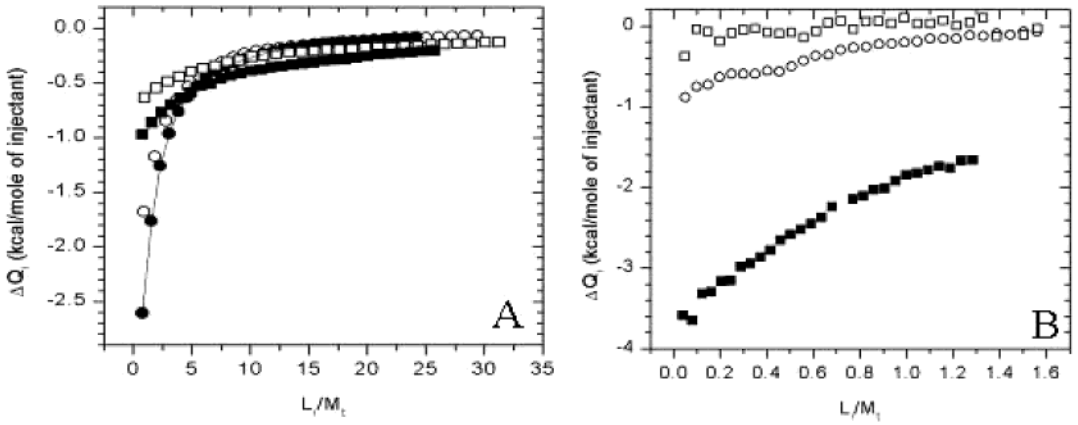

FIGURE 4: Binding of propofol and volatile anesthetics. (A) ΔQ_i valuesof binding of halothane (■) and desflurane (●) are plotted as functions of the mole ratio of drug/BSA. After the complete titration of propofol (to 0.13 mM), a second syringe filled with an aqueous solution of either halothane (□) or desflurane (○) was then used to titrate BSA in the presence of propofol. (B) ΔQ_i values of binding of propofol (■) are plotted as functions of the mole ratio of drug/BSA. After the titration of either halothane (□) to 2.9 mM or desflurane (○) to 2.7 mM, a second syringe filled with an aqueous solution of propofol (0.8 mM) was then used to titrate the BSA.

desflurane site, leaving residual binding to the low-affinity sites, mainly intact (see the caption of Figure 5), consistent with mutually exclusive binding to the former site. Similar results were obtained with HSA (not shown). These results suggest that the high-affinity desflurane-binding site overlaps the propofol-binding site located in subdomain IIIA (*20*).

To assess the molecular nature of the changes to protein and anesthetic that occur upon binding, the differences in heat capacity (ΔC_p) were also measured. ΔC_p values are calculated from the slopes of ΔH, fit to its linear relationship with temperature (Table 1). Over the range of 15−25 °C or 10−35 °C, these slopes were negative, indicating that the heat capacities of the solutions had decreased upon binding (for example, see Figure 6). Similar values were obtained when the desflurane-binding data were analyzed using the two classes of site model (Table 2). These measured values are consistently more negative than those predicted by empirical calculations, which are based on shielding of hydrophobic areas of the drug from solvent water, whether or not a penalty for burying polar surface areas is included (*26*, *27*).

This discordance between the calculated and observed changes in heat capacities suggested that solvent restructuring is propagated beyond the binding site itself; such changes may be associated with overall stabilization of the native protein conformation. To examine this possibility, we compared the effects of the closely related haloethers, desflurane, isoflurane, and enflurane, on the stability of BSA to chemical denaturation. Previous work had demonstrated that halothane stabilizes BSA to thermal denaturation, as reflected by the higher melting temperatures and greater excess heat capacities of the drug/protein complex (*30*, *31*). Our results are consistent with these observations (Figure 7). The effects of GdmHCl on intrinsic tryptophan fluorescence, however, did not conform to a simple two-state model of native and denatured protein; rather, broad shallow transitions preceded and followed the main transition, except for desflurane, which had a steeper slope (Figure 7). A total of 2.5 mM of the haloethers stabilized serum albumin, as indicated by the significant shifts in the main transition midpoints (Figure 7). These complex effects are not unexpected, because serum albumin, like most proteins, does not exhibit a single unfolding transition (*32*, *33*), and so differential effects on individual subdomains would not be surprising.

The negative ΔC_p and increased native protein stability associated with binding are consistent with desolvation of

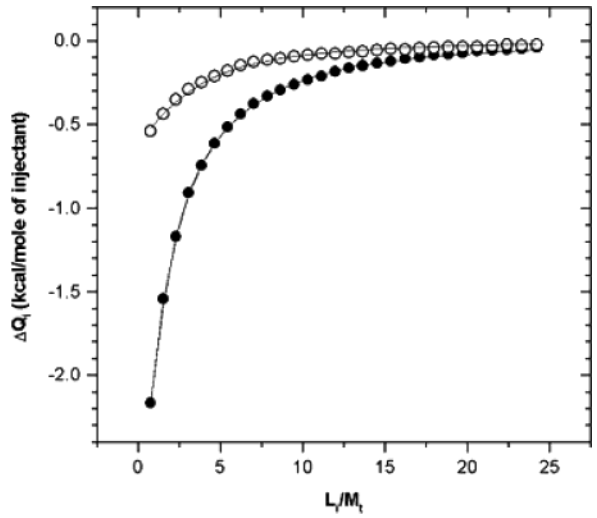

FIGURE 5: Effects of saturating propofol concentration on desflurane binding. ΔQ_i values of binding of desflurane (○ and ●) are plotted as functions of the mole ratio of drug/BSA. BSA (0.15 mM) was dissolved either in buffer (●) or in buffer containing 0.82 mM propofol (○). Binding data obtained in the absence of propofol were fit to a two classes of site model (eq 8) [$n_1 = 1$ and $n_2 = 2$; $K_1 = 21\,650 \pm 7658$ and $K_2 = 1333 \pm 94.05$; $\Delta H_1 = -2988 \pm 263.5$ and $\Delta H_2 = -3878 \pm 104.8$; and $\Delta S_1 = 9.814$ and $\Delta S_2 = 1.307$], whereas the results obtained in the presence of a saturated aqueous propofol solution were best fit using a one class of sites model (eq 1) [$n = 2$; $K = 1659 \pm 56.86$; $\Delta H = -1732 \pm 28.70$; and $\Delta S = 8.825$].

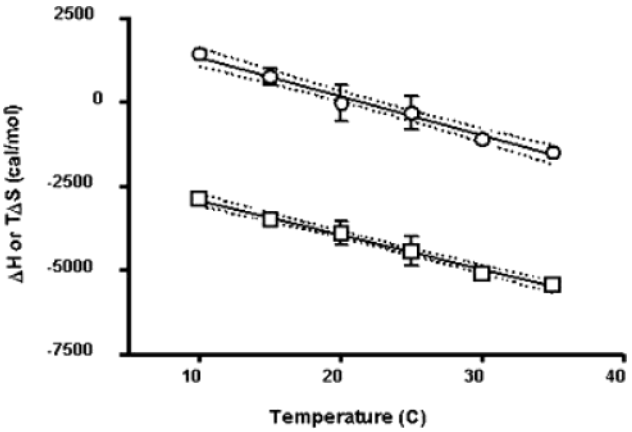

FIGURE 6: Effects of temperature on ΔH_{obs} for binding of isoflurane to BSA. Isoflurane was titrated into a buffered solution of 0.15 mM BSA at temperatures ranging from 10−35 °C. Each point is the mean ± SD of ΔH_{obs} (□) or $T\Delta S_{obs}$ (○) determined from multiple independent binding curves. (- - -) represents 95% CI.

hydrophobic surfaces of the drug and protein. To assess the solvent contribution to ΔG_{obs}, we conducted ITC measurements in solutions of D_2O and compared these to carefully matched H_2O solutions. If the role of solvent is critical, then the ratios of the thermodynamic parameters should be significantly affected, because D_2O is more strongly deuterium-bonded than the equivalent hydrogen-bonded network of water (*34*).

The ΔQ_i values for binding of isoflurane and desflurane were consistently smaller in D_2O compared with those obtained in H_2O. The results (Table 2) show a reduction of ΔH_{obs} for both desflurane and isoflurane. Despite this decrement, K increased somewhat because of a significant increase in ΔS_{obs}. These results are consistent with the release

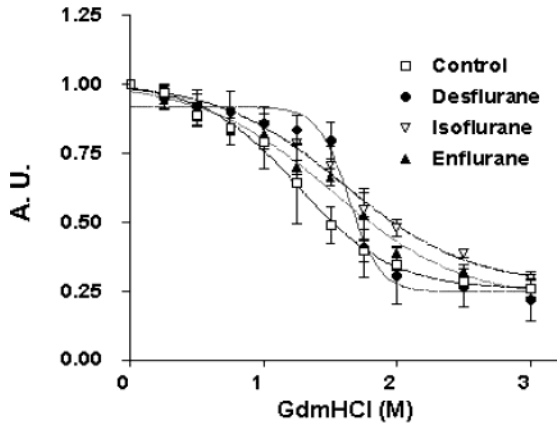

FIGURE 7: Effects of anesthetics on the stability of BSA to chemical denaturation. The intrinsic fluorescence of 100 nM defatted BSA is measured as a function of [GdmHCl] (□) and compared to protein equilibrated with 2.5 mM of either desflurane (●), isoflurane (▽), or enflurane (▲) at 20 °C. The results are plotted as the mean ± SD of two independent determinations. A sigmoidal dose response relation was fit to each data set. The transition midpoints in molar [GdmHCl] concentrations for the control, desflurane, isoflurane, and enflurane are 1.27 ± 0.09, 1.64 ± 0.05 ($p < 0.002$), 1.59 ± 0.09 ($p < 0.037$), and 1.51 ± 0.08 ($p < 0.148$), respectively.

of weakly bound water in the binding of volatile anesthetics to serum albumin.

DISCUSSION

The results of this study demonstrate that ΔH contributes largely to the free-energy change associated with binding of volatile anesthetics to serum albumin. Binding also produces a significant decrease in heat capacity and stabilizes the native state of the protein. The results suggest that the solvent, hydrating the anesthetic and protein, is released upon formation of the complex. This idea is supported by isotopic substitution that demonstrates that solvent restructuring contributes to both enthalpy and entropy, leading to the conclusion that much of the anesthetic-binding free energy derives from the reordering of water molecules solvating the anesthetic and its binding site.

The anesthetic affinities measured here agree well with those obtained using other techniques including photoaffinity labeling (*12*−*14*, *35*), ^{19}F NMR spectroscopy (*17*, *36*, *37*), quenching of tryptophan fluorescence (*35*, *38*), tryptophan fluorescence anisotropy, thermal denaturation (*39*), and zonal elution chromatography (*16*, *19*).[2] Moreover, photoaffinity labeling and NMR experiments have shown that halothane, isoflurane, enflurane, and sevoflurane compete for a limited number of binding sites on albumin (*14*).

A recent crystallographic study of HSA (*20*) has helped clarify where halothane and propofol bind and, by extension, other volatile agents as well. Serum albumin is a globular α-helical protein consisting of multiple subdomains each of which is capable of binding one or more fatty acids and a wide range of other hydrophobic compounds (*40*−*44*). Native crystals of fatty-acid-free HSA, exposed to low

[2] The compounds used here, as in most anesthetic-binding studies, are racemic mixtures. Which stereoisomers bind best under our conditions is not known, and so the binding constants that we report remain apparent. Nonetheless, previous work suggests only slight differences in the binding of isoflurane stereoisomers to serum albumin (*12*, *14*, *37*).

halothane partial pressures (5 atm %, corresponding to an aqueous concentration of ~2.6 mM), bind three molecules of anesthetic distributed between two distinct sites per molecule of HSA (*20*). At higher partial pressures, halothane occupies five additional sites. At the lower partial pressures, which represent the maximum concentrations achieved in our titration measurements, one halothane molecule is bound in subdomain IIIA, where it makes close contacts with mostly hydrophobic residues, overlapping one of two propofol-binding sites; at these partial pressures, two other halothanes are located in a groove between subdomains IIA and B, in contact with nonpolar and polar side chains. These results are consistent with fluorescence-quenching and mutagenesis study that independently identified these same sites as accounting for "high-affinity" anesthetic binding to serum albumin (*35*). Similar binding sites, containing a mixture of hydrophobic and polar residues, have been described for the complex of the anesthetic, bromoform, with firefly luciferase (*45*).

As in previous studies of serum albumin (*36*, *38*), we observe competition among the anesthetic compounds that are consistent with these crystallographic data. We have extended this work to show that desflurane and propofol also compete with halothane, isoflurane, enflurane, and sevoflurane. Given that propofol, at the concentrations that we employed, occupies only one of the high-affinity halothane sites (*20*), it can be inferred that all of the drugs tested compete for at least one common site located in subdomain IIIA. This is most clear for desflurane, where high-affinity binding of this volatile drug is greatly reduced by high concentrations of propofol (0.82 mM). The high affinity of desflurane for this site also suggests that a significant fraction of the available serum albumin is bound to desflurane at its clinically useful concentrations, which could affect the free fractions of other drugs normally bound to this protein and circulating in the plasma.

van der Waals interactions between the drug and protein, as well as changes in solvent structure (discussed below), could underlie the favorable enthalpic changes measured here. A previous study of the anesthetic gas, xenon, suggested that short range interactions, involving London dispersion forces and a charge induced dipole, could account for the binding free energy of this highly polarizable gas to hydrophobic sites in metmyoglobin (*48*). Measurements and predictions of partial charge distributions indicate that haloalkane and haloether anesthetics, unlike xenon, have significant dipole moments (*49*), suggesting that favorable dipole−dipole and dipole induced dipole interactions could contribute to ΔH. The net dipole moments of the individual anesthetics, however, are not predictive of K_{obs} or ΔH_{obs} for binding to serum albumin nor are other parameters, such as molecular volumes, surface areas, or oil/water partition coefficients; on the other hand, the lipole moment, the lipophilicity vector across the entire molecule (comparable to the Eisenberg hydrophobic moment), is weakly correlated ($r = 0.65$). Thus, no conclusive structural pattern or single molecular property accounts for differences in ΔH_{obs} or ΔG_{obs} among the drugs.

The energetics of the binding described here are similar to those reported for chloroform binding to serum albumin. Binding of this haloalkane is also exothermic, with ΔH_{obs} making a major contribution to binding free energy (*22*). Enthalpy also contributes favorably to the free energy of inhibition of firefly luciferase by a wide range of general anesthetic agents (*46*). For example, the value obtained for halothane (−4.3 kcal/mol) is comparable to the binding enthalpies measured for HSA (−4.9) and BSA (−6.2) (Table 1). Similarly, halothane and isoflurane inhibition of acetylcholine-regulated chloride channels (*47*) is associated with apparent enthalpy changes (−4.8 and −5.7 kcal/mol), close to those reported here (Table 1).

The contribution of ΔS_{obs} to the binding free energies is variable and relatively small in magnitude, $-T\Delta S \sim -1600$ to +2800 cal/mol, with favorable entropy contributions observed for desflurane and isoflurane. In the case of desflurane, the increased entropy accounts for significantly stronger binding. In contrast, the unfavorable entropic term for halothane gives rise to a reduced K despite a strong enthalpic contribution. Comparing desflurane, isoflurane, enflurane, and halothane yields a positive correlation between $-T\Delta S$ and ΔG (slope $= 1.6 \pm 0.24$ and $r^2 = 0.63$) (Figure 2). It is interesting to note that the binding free energy correlates better with the increment in $-T\Delta S$ rather than ΔH, in contrast to luciferase inhibition (*46*). This inverse relationship between ΔH and $-T\Delta S$ is consistent with the concept that stronger intrinsic interactions have higher entropy costs (*50*).[3]

What underlies ΔS_{obs}? Burying the anesthetics in an apolar cavity should increase solvent entropy, which could account for − 6.2 to −7.7 kcal/mol through the reordering of water at these temperatures (*51*) (assuming up to 25 cal/mol per A^2 of nonpolar surface area), but losses of translational and rotational entropy of the drug are on this same order (*52*). Moreover, binding also increases internal degrees of freedom through new vibrational modes, and these are likely to be on the order of −5 to −10 kcal/mol (*53*). Thus, offsetting positive and negative terms are likely to contribute to ΔS_{obs}.

The negative ΔC_p measured here suggests a burial of nonpolar surfaces (*54*, *55*). Reducing exposure to water should increase its disorder and increase ΔS, favoring a compact folded state of the protein, which is consistent with stabilization of BSA by these compounds against chemical (Figure 4) and thermal denaturation (*30*, *31*, *39*). This is also supported by hydrogen/tritium exchange studies (*12*, *35*) that yield comparable degrees of stabilization.

The decreased heat capacities and the increased conformational stabilities suggest that binding of anesthetics may modify albumin structure, producing a distinct conformational change. Alternatively, anesthetics could alter internal protein dynamics, decreasing the exposure of hydrophobic groups to water by reducing main- and side-chain motions. The former interpretation seems unlikely, given that major changes in the main-chain conformation are not observed for binding of halothane as determined by CD spectroscopy (*39*) or by X-ray crystallography (*20*). More subtle effects on main- and side-chain dynamics, however, are supported by the decreased rates of hydrogen/tritium exchange from albumin bound to halothane or isoflurane (*12*, *35*) and by enhanced fluorescence anisotropy of its tryptophan side

[3] The incremental loss of translational entropy for this series of compounds, estimated from the relation $\Delta\Delta S = \ln(M_1/M_2)^{3/2}$, could account for up to 10−20% of the decrement in ΔS between desflurane and sevoflurane (Figure 2).

Table 3: Comparison of the Thermodynamic Parameters of Anesthetic Binding to BSA in the Presence of H_2O or D_2O[a]

drug	K_{H_2O}	K_{D_2O}	ΔG_{H_2O}	ΔG_{D_2O}	ΔH_{H_2O}	ΔH_{D_2O}	ΔS_{H_2O}	ΔS_{D_2O}
desflurane	3398 ± 542	5910 ± 375**	−4749 ± 149	−5056 ± 179	−3269 ± 153	−2835 ± 282**	4.96 ± 0.63	7.58 ± 0.96***
isoflurane	1387 ± 64	1594 ± 138	−4216 ± 111	−4286 ± 111	−3718 ± 67	−3583 ± 67*	1.7 ± 0.3	2.4 ± 0.4**

[a] Apparent association constants K and the binding enthalpies ΔH were determined at 20 °C from fits to the data of a single class, noninteracting binding sites model (eq 1). The results are presented as the mean ± SD of 3 and 4 independent titrations for desflurane and isoflurane, respectively. Significantly different from H_2O. *, $p < 0.05$; **, $p < 0.02$; and ***, $p < 0.002$.

Scheme 1: Cycle of Solvation and Binding

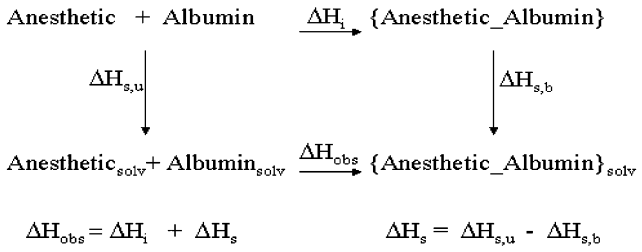

chains (*39*). On the other hand, differences in the calculated temperature factors at the halothane-binding sites suggest little change in dynamics (*20*). It should be noted, however, that serum albumin fails to crystallize in the presence of halothane, so that the diffraction data were only obtained from native crystals exposed to anesthetic. Overall, these results imply that the internal dynamics of the protein are reduced through dissipation of the anesthetic-binding free energy, as previously suggested (*39*). These changes could diminish access of aqueous solvent to the interior of the protein, effectively shielding hydrophobic residues and accounting for the increased stability and negative ΔC_p that we observe.

The effects of substituting D_2O for H_2O further support the idea that solvent reordering makes an important contribution to the anesthetic-binding free energy. The results show small but significant decreases of ΔH_{obs} and substantial increases of ΔS_{obs} for binding of desflurane and isoflurane to BSA. A consideration of water in the ligand-binding reaction is required to understand what underlies the effect. As described by Chervenak and Toone (*56*), the contribution of solvent to the binding enthalpy or entropy can be depicted by a simple thermodynamic cycle (Scheme 1). Here, binding of the desolvated states of anesthetic and albumin and their complex are compared to fully solvated free components and their complex. ΔH_{obs} of binding in aqueous solution is equal to the sum of the binding enthalpies because of intrinsic attractions between the unsolvated anesthetic and the protein (ΔH_i) and the enthalpic differences in solvating the free and bound components (ΔH_s). Thus, the contribution of solvent to ΔH_{obs} arises from the difference between $\Delta H_{s/u}$ and $\Delta H_{s/b}$, which derives from differences in the structure and stability of bulk and interfacial water (*57*).

Because ΔH_i appears to involve mainly van der Waals interactions between anesthetics and albumin, it is not expected to be different in the two solvents. Thus, the main effect should be on ΔH_s. Increasing the stability of the free components in D_2O relative to the bound components should reduce the contribution of $\Delta H_{s/u}$ to ΔH_s and thus decrease the magnitude of ΔH_{obs}.[4] This interpretation is supported by favorable changes in the enthalpy associated with transfer of nonpolar compounds from the gaseous or solid state to D_2O compared to H_2O (*58*−*60*). The apparent stabilization by D_2O of the unbound state relative to the bound state implies that the release of water from the solvated drug and binding site interface contributes favorably to the enthalpy. While the absolute magnitude of the deuterium effects are small (4 and 14%), these are close to the difference in intermolecular hydrogen-bonding energies between D_2O and H_2O, estimated to be ∼10% greater for D_2O compared to H_2O (*61*). This would suggest that solvent restructuring is a major contributor to the apparent binding enthalpy, at least on the order of ΔH_i. While no major differences are observed in the water strongly bound to HSA and the HSA/halothane complex (*20*), it is the loosely bound water, invisible in these structures, that is likely to be released.

[4] On the other hand, increases in $\Delta H_{s/b}$, could in theory produce comparable decreases in ΔH_{obs}, but differences here would require a direct participation of water in forming the complex, which is unlikely for isoflurane and desflurane, and is not observed in the structures of HSA bound with halothane (*20*).

ACKNOWLEDGMENT

The work in the authors' laboratory is supported by NIH Grant GM-60376. We also acknowledge the helpful comments and suggestions of Dr. James Dilger.

REFERENCES

1. Dilger, J. (1994) Basic Pharmacology of Inhalational Anesthetic Agents, in *The Pharmacologic Basis of Anesthesiology* (Bowdle, T., Horita, A., and Kharasch, E. D., Eds.) pp 497−521, Churchill Livingstone, New York.
2. Franks, N. P., and Lieb, W. R. (1994) Molecular and cellular mechanisms of general anaesthesia, *Nature 367*, 607−614.
3. Eckenhoff, R. G., and Johansson, J. S. (1997) Molecular interactions between inhaled anesthetics and proteins, *Pharmacol. Rev. 49*, 343−367.
4. Cafiso, D. S. (1998) Effects of halothane on μ opioid binding in SH-SY5Y cells, *Toxicol. Lett. 100* and *101*, 431−439.
5. Cantor, R. S. (2001) Breaking the Meyer−Overton rule: Predicted effects of varying stiffness and interfacial activity on the intrinsic potency of anesthetics, *Biophys. J. 80*, 2284−2297.
6. Cantor, R. S. (1997) The lateral pressure profile in membranes: A physical mechanism of general anesthesia, *Biochemistry 36*, 2339−2344.
7. Franks, N. P., and Lieb, W. R. (1993) Selective actions of volatile general anaesthetics at molecular and cellular levels, *Br. J. Anesthes. 71*, 65−76.
8. Yamakura, T., Bertaccini, E., Trudell, J. R., and Harris, R. A. (2001) Anesthetics and ion channels: Molecular models and sites of action, *Annu. Rev. Pharmacol. Toxicol. 41*, 23−51.
9. Eckenhoff, R. G. (2001) Promiscuous ligands and attractive cavities: How do the inhaled anesthetics work? *Mol. Interv. 1*, 258−268.
10. Trudell, J. R., and Bertaccini, E. (2002) Molecular modelling of specific and non-specific anaesthetic interactions, *Br. J. Anaesth. 89*, 32−40.
11. Rebecchi, M. J., and Pentyala, S. N. (2002) Anaesthetic actions on other targets: Protein kinase C and guanine nucleotide-binding proteins, *Br. J. Anaesth. 89*, 62−78.

12. Eckenhoff, R. G., and Tanner, J. W. (1998) Differential halothane binding and effects on serum albumin and myoglobin, *Biophys. J. 75*, 477−483.
13. Eckenhoff, R. G. (1996) Amino acid resolution of halothane binding sites in serum albumin, *J. Biol. Chem. 271*, 15521−15526.
14. Eckenhoff, R. G., and Shuman, H. (1993) Halothane binding to soluble proteins determined by photoaffinity labeling, *Anesthesiology 79*, 96−106.
15. Johansson, J. S. (1997) Binding of the volatile anesthetic chloroform to albumin demonstrated using tryptophan fluorescence quenching, *J. Biol. Chem. 272*, 17961−17965.
16. Liu, R., Pidikiti, R., Ha, C. E., Petersen, C. E., Bhagavan, N. V., and Eckenhoff, R. G. (2002) The role of electrostatic interactions in human serum albumin binding and stabilization by halothane, *J. Biol. Chem. 277*, 36373−36379.
17. Dubois, B. W., and Evers, A. S. (1992) ^{19}F NMR spin−spin relaxation (T2) method for characterizing volatile anesthetic binding to proteins. Analysis of isoflurane binding to serum albumin, *Biochemistry 31*, 7069−7076.
18. Yoshida, T., Tanaka, M., Mori, Y., and Ueda, I. (1997) Negative entropy of halothane binding to protein: ^{19}F NMR with a novel cell, *Biochim. Biophys. Acta 1334*, 117−122.
19. Chan, K., Meng, Q. C., Johansson, J. S., and Eckenhoff, R. G. (2002) Low-affinity analytical chromatography for measuring inhaled anesthetic binding to isolated proteins, *Anal. Biochem. 301*, 308−313.
20. Bhattacharya, A. A., Curry, S., and Franks, N. P. (2000) Binding of the general anesthetics propofol and halothane to human serum albumin. High resolution crystal structures, *J. Biol. Chem. 275*, 38731−38738.
21. Johansson, J. S., Scharf, D., Davies, L. A., Reddy, K. S., and Eckenhoff, R. G. (2000) A designed four-α-helix bundle that binds the volatile general anesthetic halothane with high affinity, *Biophys. J. 78*, 982−993.
22. Ueda, I., and Yamanaka, M. (1997) Titration calorimetry of anesthetic−protein interaction: Negative enthalpy of binding and anesthetic potency, *Biophys. J. 72*, 1812−1817.
23. Pentyala, S. N., Sung, K., Chowdhury, A., and Rebecchi, M. J. (1999) Volatile anesthetics modulate the binding of guanine nucleotides to the α subunits of heterotrimeric GTP binding proteins, *Eur. J. Pharmacol. 384*, 213−222.
24. Chervenak, M. C., and Toone, E. J. (1994) A direct measure of the contribution of solvent reorganization to the enthalpy of ligand-binding, *J. Am. Chem. Soc. 116*, 10533−10539.
25. Pedretti, A., Villa, L., and Vistoli, G. (2002) VEGA: A versatile program to convert, handle, and visualize molecular structure on Windows-based PCs, *J. Mol. Graphics Modell. 21*, 47−49.
26. Livingstone, J. R., Spolar, R. S., and Record, M. T., Jr. (1991) Contribution to the thermodynamics of protein folding from the reduction in water-accessible nonpolar surface area, *Biochemistry 30*, 4237−4244.
27. Spolar, R. S., Livingstone, J. R., and Record, M. T., Jr. (1992) Use of liquid hydrocarbon and amide transfer data to estimate contributions to thermodynamic functions of protein folding from the removal of nonpolar and polar surface from water, *Biochemistry 31*, 3947−3955.
28. Gaillard, P., Carrupt, P. A., Testa, B., and Boudon, A. (1994) Use of liquid hydrocarbon and amide transfer data to estimate contributions to thermodynamic functions of protein folding from the removal of nonpolar and polar surface from water, *J. Comput.-Aided Mol. Des. 8*, 83−96.
29. Pedretti, A., Villa, L., and Vistoli, G. (2002) *J. Med. Chem. 45*, 1460−1465.
30. Tanner, J. W., Eckenhoff, R. G., and Liebman, P. A. (1999) Halothane, an inhalational anesthetic agent, increases folding stability of serum albumin, *Biochim. Biophys. Acta 1430*, 46−56.
31. Tanner, J. W., Liebman, P. A., and Eckenhoff, R. G. (1998) Volatile anesthetics alter protein stability, *Toxicol. Lett. 100* and *101*, 387−391.
32. Shrake, A., and Ross, P. D. (1990) Ligand-induced biphasic protein denaturation, *J. Biol. Chem. 265*, 5055−5059.
33. Farruggia, B., Rodriguez, F., Rigatuso, R., Fidelio, G., and Pico, G. (2001) The participation of human serum albumin domains in chemical and thermal unfolding, *J. Protein Chem. 20*, 81−89.
34. Rekharsky, M. V., and Inoue, Y. (2002) Solvent and guest isotope effects on complexation thermodynamics of α-, β-, and 6-amino-6-deoxy-β-cyclodextrins, *J. Am. Chem. Soc. 124*, 12361−12371.
35. Eckenhoff, R. G., Petersen, C. E., Ha, C. E., and Bhagavan, N. V. (2000) Inhaled anesthetic binding sites in human serum albumin, *J. Biol. Chem. 275*, 30439−30444.
36. Dubois, B. W., Cherian, S. F., and Evers, A. S. (1993) Volatile anesthetics compete for common binding sites on bovine serum albumin: A ^{19}F NMR study, *Proc. Natl. Acad. Sci. U.S.A. 90*, 6478−6482.
37. Xu, Y., Tang, P., Firestone, L., and Zhang, T. T. (1996) ^{19}F nuclear magnetic resonance investigation of stereoselective binding of isoflurane to bovine serum albumin, *Biophys. J. 70*, 532−538.
38. Johansson, J. S., Eckenhoff, R. G., and Dutton, P. L. (1995) Binding of halothane to serum albumin demonstrated using tryptophan fluorescence, *Anesthesiology 83*, 316−324.
39. Johansson, J. S., Zou, H., and Tanner, J. W. (1999) Bound volatile general anesthetics alter both local protein dynamics and global protein stability, *Anesthesiology 90*, 235−245.
40. He, X. M., and Carter, D. C. (1992) Atomic structure and chemistry of human serum albumin, *Nature 358*, 209−215.
41. Carter, D. C., and He, X. M. (1990) Structure of human serum albumin, *Science 249*, 302−303.
42. Curry, S., Mandelkow, H., Brick, P., and Franks, N. (1998) Crystal structure of human serum albumin complexed with fatty acid reveals an asymmetric distribution of binding sites, *Nat. Struct. Biol. 5*, 827−835.
43. Curry, S., Brick, P., and Franks, N. P. (1999) Fatty acid binding to human serum albumin: New insights from crystallographic studies, *Biochim. Biophys. Acta 1441*, 131−140.
44. Sugio, S., Kashima, A., Mochizuki, S., Noda, M., and Kobayashi, K. (1999) Crystal structure of human serum albumin at 2.5 Å resolution, *Protein Eng. 12*, 439−446.
45. Franks, N. P., Jenkins, A., Conti, E., Lieb, W. R., and Brick, P. (1998) Structural basis for the inhibition of firefly luciferase by a general anesthetic, *Biophys. J. 75*, 2205−2211.
46. Dickinson, R., Franks, N. P., and Lieb, W. R. (1993) Thermodynamics of anesthetic/protein interactions. Temperature studies on firefly luciferase, *Biophys. J. 64*, 1264−1271.
47. Dickinson, R., Lieb, W. R., and Franks, N. P. (1995) The effects of temperature on the interactions between volatile general anaesthetics and a neuronal nicotinic acetylcholine receptor, *Br. J. Pharmacol. 116*, 2949−2956.
48. Trudell, J. R., Koblin, D. D., and Eger, E. I., II (1998) A molecular description of how noble gases and nitrogen bind to a model site of anesthetic action, *Anesth. Analg. 87*, 411−418.
49. Trudell, J. R., and Bertaccini, E (2002) Molecular modelling of specific and non-specific anaesthetic interactions, *Br. J. Anesth. 89*, 32−40.
50. Borea, P. A., Dalpiaz, A., Varani, K., Gilli, P., and Gilli, G. (2000) Can thermodynamic measurements of receptor binding yield information on drug affinity and efficacy? *Biochem. Pharmacol. 60*, 1549−1556.
51. Chothia, C. (1974) Hydrophobic bonding and accessible surface area in proteins, *Nature 248*, 338−339.
52. Doty, P., and Myers, G. E. (1953) Thermodynamics of the association of insulin molecules, *Discuss. Faraday Soc. 13*, 51−58.
53. Tidor, B., and Karplus, M. (1994) The contribution of vibrational entropy to molecular association. The dimerization of insulin, *J. Mol. Biol. 238*, 405−414.
54. Cooper, A. (1999) Thermodynamic analysis of biomolecular interactions, *Curr. Opin. Chem. Biol. 3*, 557−563.
55. Jelesarov, I., and Bosshard, H. R. (1999) Isothermal titration calorimetry and differential scanning calorimetry as complementary tools to investigate the energetics of biomolecular recognition, *J. Mol. Recognit. 12*, 3−18.
56. Chervenak, M. C., and Toone, E. J. (1995) Calorimetric analysis of the binding of lectins with overlapping carbohydrate-binding ligand specificities, *Biochemistry 34*, 5685−5695.
57. Muller, N. (1990) Search for a relaistic view of hydrophobic effects, *Acc. Chem. Res. 23*, 23−28.
58. Kresheck, G. C., Scneider, H., and Scheraga, H. A. (1965) The effect of D_2O on the thermal stability of proteins. Thermodynamic parameters for the transfer of model compounds from H_2O to D_2O, *J. Phys. Chem. 69*, 3132−3144.

59. Ben-Naim, A., Wilf, J., and Yaacobi, M. (1973) Hydrophobic interaction in light and heavy water, *J. Phys. Chem. 77*, 95−102.
60. Lopez, M. M., and Makhatadze, G. I. (1998) Solvent isotope effect on thermodynamics of hydration, *Biophys. Chem. 74*, 117−125.
61. Nemethy, G., and Scheraga, H. A. (1964) Structure of water and hydrophobic bonding in proteins: Thermodynamic properties of liquid deuterium oxide, *J. Chem. Phys. 41*, 680−686.
62. Liu, R., Meng, Q., Xi, J., Yang, J., Ha, C. E., Bhagavan, N. V., and Eckenhoff, R. G. (2004) Comparative binding character of two general anesthetics for sites on human serum albumin, *Biochem. J. 380*, 147−152.

BI035941D